Article

Journal of Vibration and Control
2023, Vol. 29(13-14) 3175–3185

DOI: 10.1177/10775463221092838
journals.sagepub.com/home/jvc
Sage

Kaimal spectrum based H2 optimization of tuned mass dampers for wind turbines

Somya Ranjan Patro[1], Arnab Banerjee[1], Sondipon Adhikari[2], and G. V. Ramana[1]

Abstract

The closed-form analytical expression of the objective function of a single degree of freedom system with the tuned mass damper, subjected to Gaussian white noise and Kaimal forcing spectrum, is derived implementing the H_2 optimization technique. To illustrate the procedure, a wind turbine tower with and without the tuned mass damper, subjected to wind load, has been presented. The Kaimal spectrum has been considered to model the effects of wind load. Usually, the parameters of the tuned mass damper is optimized by implementing the H_2 optimization technique on Gaussian white noise even though the system is subject to any other forcing spectrum. Obtaining an analytical closed-form expression of the objective function for a tuned mass damper system considering a real spectrum is very challenging as a real spectrum may contain fractional order of the frequency. Therefore, either objective function can be obtained numerically or an analytical form can be obtained but only for Gaussian white noise as an input forcing spectrum. To address the above-mentioned issue, in this paper, the concept of near identity spectrum is introduced to idealize the Kaimal spectrum with high accuracy from which a closed-form expression of the objective function can be established. Further, histogram plots of the response reduction have been made to show a comparison between the tuned mass damper system optimized with Gaussian white noise and the Kaimal spectrum. The results showed that the displacement response of the tuned mass damper system subjected to the Kaimal spectrum yields better performance if it is optimized according to the Kaimal spectrum rather than Gaussian white noise and vice versa.

Keywords

Gaussian white noise, Kaimal spectrum, near identity spectrum, offshore wind turbine, H_2 optimization

1. Introduction

A tuned mass damper (TMD) is a vibration control device which can be attached to a vibrating member (primary system) subjected to the dynamic forces or base excitation. A mass connected by a parallel spring and dashpot element with the primary system is the most common form of a TMD and was first proposed by Ormondroyd, (1928). The parameters of a TMD, that is, spring stiffness and damping coefficient can be obtained by implementing two analytical optimization techniques, namely H_∞ and H_2 optimization.

The H_∞ optimization technique can be used to estimate the optimum parameters when the primary system is subjected to harmonic force/motion (Hahnkamm 1933; Brock 1946; Snowdon 1974; Warburton 1982). Minimization of the maximum amplitude magnification factor (called H_∞ norm) of the primary system is the key principle of the H_∞ optimization technique (Nishihara and Matsuhisa 1997; Ren 2001; Liu and Liu 2005; Wong and Cheung 2008; Cheung and Wong 2009). Den Hartog (1985) derived the optimum parameters of the TMD system based on the fixed point theory for minimizing the maximum vibration velocity response of a single degree of freedom (SDOF) system under harmonic excitation. Anh and Nguyen (2014) proposed an approach to determine the approximate analytical solutions for the H_∞ optimization of the dynamic vibration absorber (DVA) attached to the damped primary structure subjected to force excitation by replacing with an equivalent undamped structure. A closed-form expression

[1]Department of Civil Engineering, Indian Institute of Technology Delhi, New Delhi, India
[2]James Watt School of Engineering, The University of Glasgow, Glasgow, UK

Received: 26 November 2021; revised: 27 February 2022; accepted: 22 March 2022

Corresponding author:
Arnab Banerjee, Assistant Professor, Department of Civil Engineering, Indian Institute of Technology Delhi, Hauz Khas, New Delhi 110016, India.
Email: abanerjee@civil.iitd.ac.in

of the optimum parameters of a TMD can be obtained using the H_∞ optimization technique if and only if damping is not considered in the primary system (Ioi and Ikeda 1978; Randall et al., 1981; Thompson 1981; Soom and Lee 1983). For damped primary systems, several numerical and series solutions have been proposed for obtaining the optimum parameters as given in the state-of-the-art (Sekiguchi and Asami 1984; Yamaguchi and Harnpornchai 1993; Tsai and Lin 1993; Asami Hosokawa, 1995; Zuo 2009). Liu and Coppola (2010) used numerical approaches, namely Chebyshev's equioscillation theorem to study the optimum design of the damped primary system. Chun et al. (2015) studied the H_∞ optimal design of a DVA variant for suppressing high-amplitude vibrations of damped primary systems using the diversity-guided cyclic-network-topology-based constrained particle swarm optimization (Div-CNTCPSO) technique. In contrary, the primary objective of the H_2 optimization technique is to reduce the total vibration energy of the system's overall frequency by minimizing the area under the frequency response curve (Warburton 1982; Asami et al., 1991, 2001). Several literature have proposed H_2 optimization techniques to estimate the optimum parameters of TMD systems (Adhikari et al., 2016; Asami et al., 2002; Chowdhury et al., 2021; Adhikari and Banerjee 2021). Ghosh and Basu (2007) obtained a closed-form expression for optimum tuning ratio of the damped TMD system subjected to harmonic load and GWN. Zuo (2009) conducted decentralized H_2 and H_∞ control methods to optimize the parameters of spring stiffness and damping coefficients for random and harmonic vibration. Cheung and Wong (2011) derived H_2 optimum parameters of a DVA to minimize the total vibration energy or the mean square motion of a single degree of freedom (SDOF) system under random force excitations. Chowdhury et al. (2022) compared the H_2 and H_∞ optimization methods to identify the optimal system parameters of different vibration control devices subjected to Gaussian white noise (GWN) and harmonic motion. All the studies mentioned above are conducted using GWN when the amplitude is constant over the frequency range. However, no one derived a closed-form expression of the objective function from which the optimum parameter of the TMD can be determined while the TMD is subjected to a forcing spectrum other than GWN.

Motivated from the above-mentioned research gap, in the present study, a forcing spectrum is considered in which the amplitude is variable over the frequency domain which is more realistic in nature. As an example of a real spectrum, in this study, the Kaimal spectrum is considered. The Kaimal spectrum is often used to model the effect of wind load for offshore structures, tall buildings, cable stayed bridges, transmission towers etc. (Ankireddi and Yang 1996; IEC 2005; Det 2013; Tian and Gai 2015; Li et al., 2021). Since the function of the Kaimal spectrum usually contains fractional power of excitation frequency, the use of the H_2 optimization technique to estimate closed-form expression of the objective function can sometimes be arduous (Colwell and Basu 2009). To overcome the fractional power in the spectrum, a near identity spectrum (NIS) similar to the Kaimal spectrum is proposed in this paper, which helps in omitting the fractional power of excitation frequency. Finally, a closed-form expression can be obtained for the objective function after implementation of the H_2 optimization technique. The time displacement responses have been compared between a traditional wind turbine and wind turbine attached with a TMD system. Finally, histogram plots have been made to show a comparison between the optimum parameters of the TMD system optimized for GWN and the Kaimal spectrum.

2. Methodology

2.1. Frequency Response Function

A single degree of freedom (SDOF) system equipped with a passive TMD is considered in the present study as shown in Figure 1. Since, the two degree of freedom system given in Figure 1 can be considered as the model given by Asami et al. (2002) and defining several non-dimensional parameters such as mass ratio $\left(\mu = \frac{m_2}{m_1}\right)$, natural frequency of primary system $\left(\omega_1 = \sqrt{\frac{k_1}{m_1}}\right)$, primary system damping ratio $\left(\zeta_1 = \frac{c_1}{2m_1\omega_1}\right)$, natural frequency of the TMD $\left(\omega_2 = \sqrt{\frac{k_2}{m_2}}\right)$, TMD damping ratio $\left(\zeta_2 = \frac{c_2}{2m_2\omega_2}\right)$, frequency ratio $\left(\nu = \frac{\omega_2}{\omega_1}\right)$ and non-dimensional excitation frequency $\left(\lambda = \frac{\omega}{\omega_1}\right)$, and substituting these parameters in the equation of motion of two degree of freedom system, frequency response function (FRF) can be established as

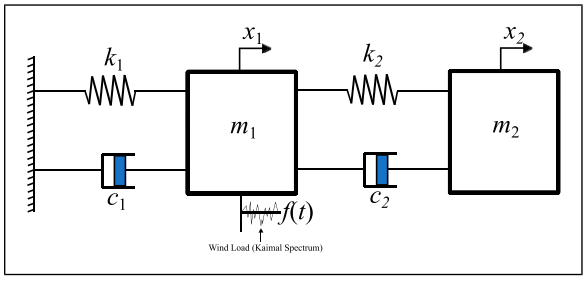

Figure 1. A tuned mass damper (TMD) system subjected to random wind load (Kaimal spectrum).

$$H(\lambda) = \frac{v^2 + (i\lambda)^2 + 2\zeta_2 v(i\lambda)}{\left(\begin{array}{c}(i\lambda)^4 + (2\zeta_1 + 2v\zeta_2 + 2\mu v\zeta_2)(i\lambda)^3 + \\ \left(1 + v^2 + \mu v^2 + 4v\zeta_1\zeta_2\right)(i\lambda)^2 + \\ \left(2\zeta_1 v^2 + 2\zeta_2 v\right)(i\lambda) + v^2\end{array}\right)} \quad (1)$$

2.2. Kaimal spectrum

Since our two degree of freedom system is subjected to wind force which is considered as random load. Thus, following the DNV code (Det 2013), the Kaimal spectrum (KS) is used to incorporate the effect of wind load. The theoretical KS for fixed point reference point in space can be written as

$$S_{uu,k}(\omega) = \frac{\sigma_U^2\left(\frac{4L_k}{\overline{U}}\right)}{\left(1 + \frac{3\omega L_k}{\pi\overline{U}}\right)^{\frac{5}{3}}} \quad (2)$$

where L_k is the integral length scale, $\overline{U}$ is the mean wind speed, σ_U is the standard deviation of mean wind speed and f is the excitation frequency in Hz. The spectral density of the turbulent thrust force on the rotor $S_{FF,wind,k}(\omega)$ following (Arany et al., 2015) can be written as

$$S_{FF,wind,k}(\omega) = \rho_a^2 \frac{D^4\pi^2}{16} C_T^2 \overline{U}^2 \sigma_U^2 \tilde{S}_{uu,k}(\omega) \quad (3)$$

where

$$\tilde{S}_{uu,k}(\omega) = \frac{S_{uu,k}(\omega)}{\sigma_U^2} \quad (4)$$

and

$$\sigma_U = I\overline{U} \quad (5)$$

where D is the diameter of the rotor, $\tilde{S}_{uu,k}(\omega)$ is the normalized Kaimal spectrum, ρ_a is the density of air, C_T is the thrust coefficient, and I is the turbulence intensity. The thrust coefficient can be estimated using (Frohboese et al., 2010) as

$$C_T = \frac{7}{\overline{U}} \quad (6)$$

Since, angular excitation frequency ω is the only variable and all other parameters can be considered as a constant. Thus, equation (3) can be written as

$$S_{FF,k}(\omega) = \frac{\alpha}{(\beta\omega + 1)^{\frac{5}{3}}} \quad (7)$$

2.3. Objective function

Since our TMD system is subjected to random load, to estimate the optimum parameters such as optimum frequency ratio (v_{opt}) and TMD damping ratio (ζ_{2opt}), the H_2 optimization technique (Asami et al., 2002) is used. In this method, standard deviation is considered as the objective function which is to be minimized. Thus, the standard deviation of displacement response can be derived following (Adhikari et al., 2016) as

$$\begin{aligned}\sigma_{xx}^2 = E\left[x^2(t)\right] = R_{xx}(0) &= \int_{-\infty}^{\infty} S_{FF}(\omega)|H(\omega)|^2 d\omega \\ &= \omega_1 \int_{-\infty}^{\infty} S_{FF}(\lambda)|H(\lambda)|^2 d\lambda\end{aligned} \quad (8)$$

For simplification, equation (7) can be written in the form

$$S_{FF,k}(\lambda) = \frac{\alpha}{(\beta\omega + 1)^{\frac{5}{3}}} = \frac{\alpha}{(\chi\lambda + 1)^{\frac{5}{3}}} \quad (9)$$

where $\chi = \beta\omega$ and $\omega = 2\pi f$. Now, substituting equation (9) in equation (8), we obtain

$$\sigma_{xx}^2 = \gamma \int_{-\infty}^{\infty} \frac{1}{(\chi\lambda + 1)^{\frac{5}{3}}} |H(\lambda)|^2 d\lambda \quad (10)$$

where, $\gamma = \alpha\omega_1$

2.4. Validation for Gaussian White Noise

When the TMD system is subjected to GWN, the power spectral density (PSD) will be considered as constant wrt λ. Thus, equation (8) can be normalized as

$$I_{\min} = \frac{\sigma_{xx}^2}{2\pi\omega_1 S_{FF,k}} = \frac{1}{2\pi} \times \int_{-\infty}^{\infty} |H(\lambda)|^2 d\lambda \quad (11)$$

where $I_{\min}$ is the performance index which is a non-dimensional form of variance. Now, to evaluate the integration of equation (11), Newland, (1993) suggested a methodology in which the integrand must be in the form of

$$H(\lambda) = \frac{B_0 + (i\lambda)B_1 + (i\lambda)^2 B_2 + \cdots (i\lambda)^{n-1} B_{n-1}}{A_0 + (i\lambda)A_1 + (i\lambda)^2 A_2 + \cdots (i\lambda)^n A_n} \quad (12)$$

Since equation (1) is a 4^{th} order polynomial of λ, substituting $n = 4$ in equation (12), we obtain

$$H(\lambda) = \frac{B_0 + i\lambda B_1 - \lambda^2 B_2 - i\lambda^3 B_3}{A_0 + i\lambda A_1 - \lambda^2 A_2 - i\lambda^3 A_3 + \lambda^4 A_4} \quad (13)$$

Now, comparing equation (1) and equation (13), we obtain the coefficients as

$$\begin{aligned} B_0 &= v^2, B_1 = 2\zeta_2 v, B_2 = 1, B_3 = 0 \\ A_1 &= 2\zeta_1 v^2 + 2\zeta_2 v \\ A_2 &= 1 + v^2 + \mu v^2 + 4v\zeta_1\zeta_2 \\ A_3 &= 2\zeta_1 + 2v\zeta_2 + 2\mu v\zeta_2 \\ A_4 &= 1 \end{aligned} \tag{14}$$

$$I_{\min} = \frac{\left\{\begin{array}{l} A_0 B_3^2 (A_0 A_3 - A_1 A_2) \\ +A_0 A_1 A_4 \left(2B_1 B_3 - B_2^2\right) \\ -A_0 A_3 A_4 \left(B_1^2 - 2B_0 B_2\right) \\ +A_4 B_0^2 (A_1 A_4 - A_2 A_3) \end{array}\right\}}{2A_0 A_4 \left(A_0 A_3^2 + A_4 A_1^2 - A_1 A_2 A_3\right)} \tag{15}$$

Figure 2 shows the contour of performance index $I_{\min}$ for different frequency ratio (v) and TMD damping ratio (ζ_2). From Figure 2, it can be observed that when a TMD is subjected to GWN having mass ratio ($\mu = 0.1$) and primary system damping ratio ($\zeta_1 = 0.01$), the optimum frequency ratio (v_{opt}) was found to be 0.93 and the optimum TMD damping ratio (ζ_{2opt}) was found to be 0.15. Equation (15) is also validated with Asami et al. (2002) for different values of mass ratio μ and primary system damping ratio ζ_1 as shown in Figure 3.

2.5. Optimization for the Kaimal spectrum

For the TMD system subjected to the Kaimal Spectrum, a closed-form equation of the objective function given in equation (8) cannot be directly obtained due to presence of fractional power of λ in the integrand. Thus, solving it numerically, a contour plot has been made for different frequency ratio (v) and TMD damping ratio (ζ_1) as shown in Figure 4. From Figure 4, it can be observed that when a TMD is subjected to the Kaimal spectrum having mass ratio ($\mu = 0.1$), primary system damping ratio ($\zeta_1 = 0.01$) and a non-dimensional parameter ($\chi = 100$), the optimum frequency ratio (v_{opt}) was found to be 0.91 and the optimum TMD damping ratio (ζ_{2opt}) was found to be 0.15. The non-dimensional parameter ($\chi = 100$) mainly depends on mean wind velocity $\overline{U}$, integral length scale L_k and natural frequency of the primary system (ω_1), and it has been observed that higher value of χ does not have a much effect in the change of optimum parameters, but for lesser of χ, the value of optimum frequency ratio (v_{opt}) tends toward optimum frequency ratio (v_{opt}) of Gaussian white noise.

2.6. Near Identity Spectrum

Now, to estimate the objective function for TMD system subjected to the Kaimal spectrum analytically, a near identity spectrum (NIS) has been established such that the power spectral density function can be written as

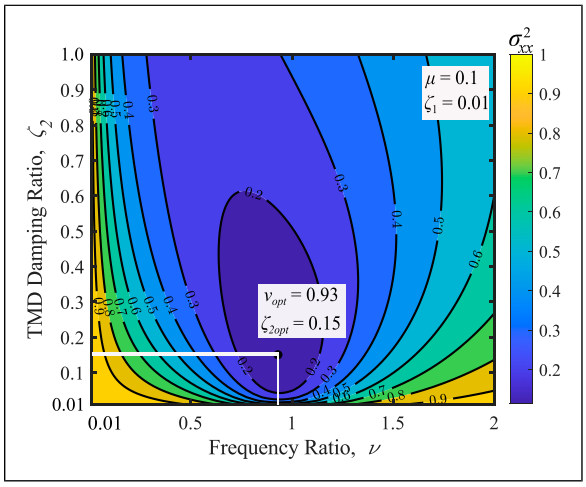

Figure 2. Contour of performance index $I_{\min}$ for different frequency ratio (v) and TMD damping ratio (ζ_2) subjected to Gaussian white noise.

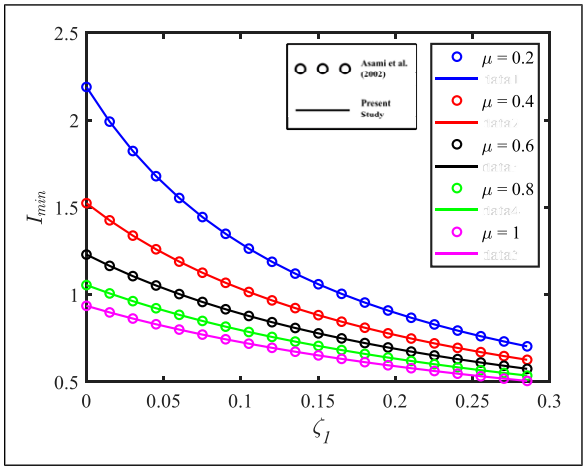

Figure 3. Validation with Asami et al. (2002) for different values of mass ratio μ and primary system damping ratio ζ_1.

$$\begin{aligned} S_{FF,k}(\lambda) &= \frac{\alpha}{(\chi\lambda + 1)^{\frac{5}{3}}} \\ \approx S_{FF,n}(\lambda) &= \frac{\alpha\delta\left(1 + \varepsilon^2\lambda^2\right)}{\left(1 + \chi^2\lambda^2\right)\left(1 + \phi^2\lambda^2\right)} \end{aligned} \tag{16}$$

where δ, ε, and ϕ are constants which depends on χ. Now, using the non-linear regression technique and curve fitting method, a relationship can be developed between δ, ε, and ϕ as a function of χ. The relationships can be expressed as

$$\delta = p_1\chi^3 + p_2\chi^2 + p_3\chi + p_4 \tag{17}$$

$$\varepsilon = q_1 \ln(\chi) + \frac{q_2}{\chi^2} + \frac{q_3}{\chi} + q_4\chi + q_5 \tag{18}$$

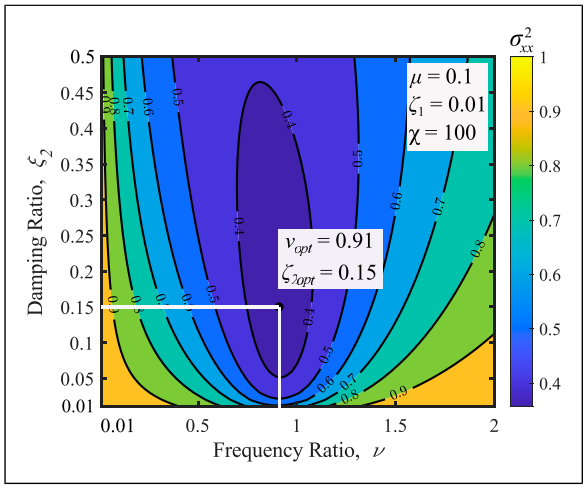

Figure 4. Contour of variance σ^2_{xx} for different frequency ratio (ν) and TMD damping ratio (ζ_2) subjected to the Kaimal spectrum. Here, the integral of equation (10) has been solved numerically to obtain the contour plot.

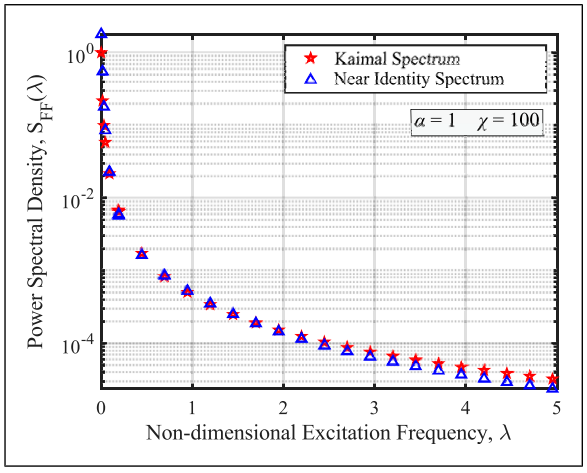

Figure 5. Comparison between the Kaimal spectrum and the near identity spectrum (NIS).

and

$$\phi = r_1 e^{(-r_2\chi)} + r_3\chi^2 + r_4\chi + r_5 \tag{19}$$

where $p_1 = 4.685 \times 10^{-8}$, $p_2 = -4.897 \times 10^{-5}$, $p_3 = 0.02069$, $p_4 = 0.9586$, $q_1 = -0.1308$, $q_2 = 1.307$, $q_3 = -2.748$, $q_4 = 0.0003$, $q_5 = 1.74$, $r_1 = -0.6364$, $r_2 = 0.2823$, $r_3 = 1.82 \times 10^{-7}$, $r_4 = -0.0001584$ and $r_5 = 0.6684$. Now, comparing equation (16) for the Kaimal spectrum and near identity spectrum in Figure 5, we can observe that the near identity spectrum almost coincides with the Kaimal spectrum and can be used as a substitute of Kaimal spectrum for further calculations. Now, to conduct H_2 optimization, substituting equation (16) in equation (8) and modifying equation (8), we get as follows

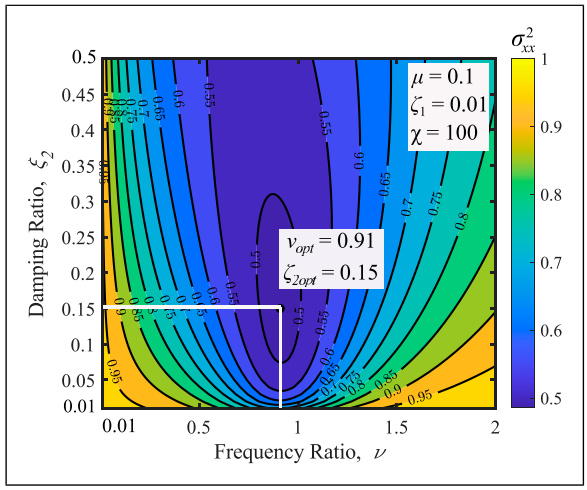

Figure 6. Contour of variance σ^2_{xx} for different frequency ratio (ν) and TMD damping ratio (ζ_2) for the near identity spectrum (NIS). Here, the integral of equation (20) has been solved analytically to obtain the contour plot.

$$\sigma_x^2 = \alpha\omega_1\delta \int_{-\infty}^{\infty} |T(\lambda)|^2 d\lambda = \frac{\pi\alpha\omega_1 M_6}{a_0\Delta_6} \tag{20}$$

where the values of $T(\lambda)$, M_6 and Δ_6 including the entire derivation of the integral in equation (20) is given in the Annexure section. Figure 6 shows a contour of variance (σ_x^2) for different frequency ratio (ν) and TMD damping ratio (ζ_1). From Figure 6, it can be observed that when a TMD is subjected to NIS having mass ratio (μ = 0.1), primary system damping ratio (ζ_1 = 0.01) and non-dimensional parameter (χ = 100), the optimum frequency ratio (ν_{opt}) was found to be 0.91 and the optimum TMD damping ratio (ζ_{2opt}) was found to be 0.15, which exactly matches with the optimum parameters of Figure 4 which provides us essential confidence to use the NIS as a substitution spectrum of the Kaimal spectrum.

3. Results and discussions

3.1. Time domain response

Using the concept of inverse fast Fourier transform, time domain wind force can be represented as sum of N sinusoids of amplitude A_i at an angular frequency ω_i having phase angle φ_i

$$F_{wind} = \sum_{i=1}^{N} A_i \sin(\omega_i t + \varphi_i) \tag{21}$$

The amplitude can be determined from the power spectral density of turbulent thrust force as

$$A = \sqrt{2S_{FF}(f)} \tag{22}$$

Now, using the MATLAB tool called ode solver and assuming the initial conditions for displacement and velocity as zero, the time domain response can be evaluated. Considering an example model of Siemens SWT-107-3.6 offshore wind turbine (Arany et al., 2015) and using the method given by Adhikari and Bhattacharya, (2011) where the entire wind turbine system can be converted into a SDOF system, the time displacement response curve has been calculated for the SDOF system, TMD optimized for GWN and TMD optimized for NIS subjected to GWN as shown inFigure 7(a to d). Similarly, all the three cases were subjected to wind load and the response was shown in Figure 8(a to d). In both Figure 7 and Figure 8 (a), the sample size of 10,000 was considered, and mean and standard deviation were plotted both for individual cases shown in Figure 7 (a to c) and Figure 8 (a to c) as well as a comparison has also been done considering all the cases as shown in Figure 7 (d) and Figure 8 (d). The wind turbine properties and the wind load properties are given in Table 1. A damping ratio (ζ_1) of 0.01 is also been considered for the wind turbine model.

3.2. Histogram plots

Although a clear understanding is formed, that is, the TMD system shows a significant reduction in displacement than the conventional SDOF system irrespective of loading condition, a clear comparison between the TMD GWN and

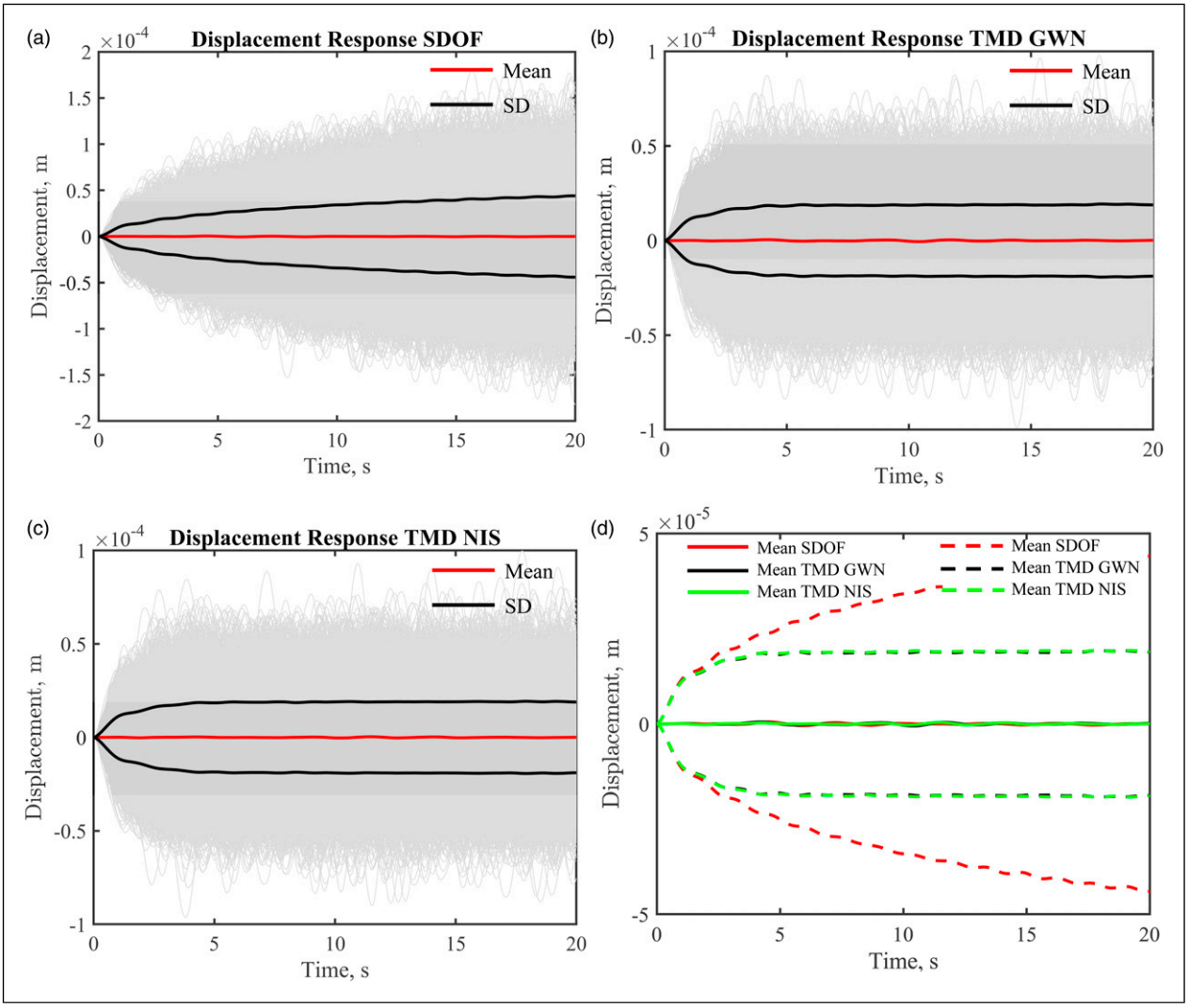

Figure 7. (a), (b) and (c) Time displacement curve including mean and standard deviation for SDOF, TMD optimized for GWN and TMD optimized for NIS subjected to GWN and (d) mean and standard deviation comparison between all the three cases subjected to GWN.

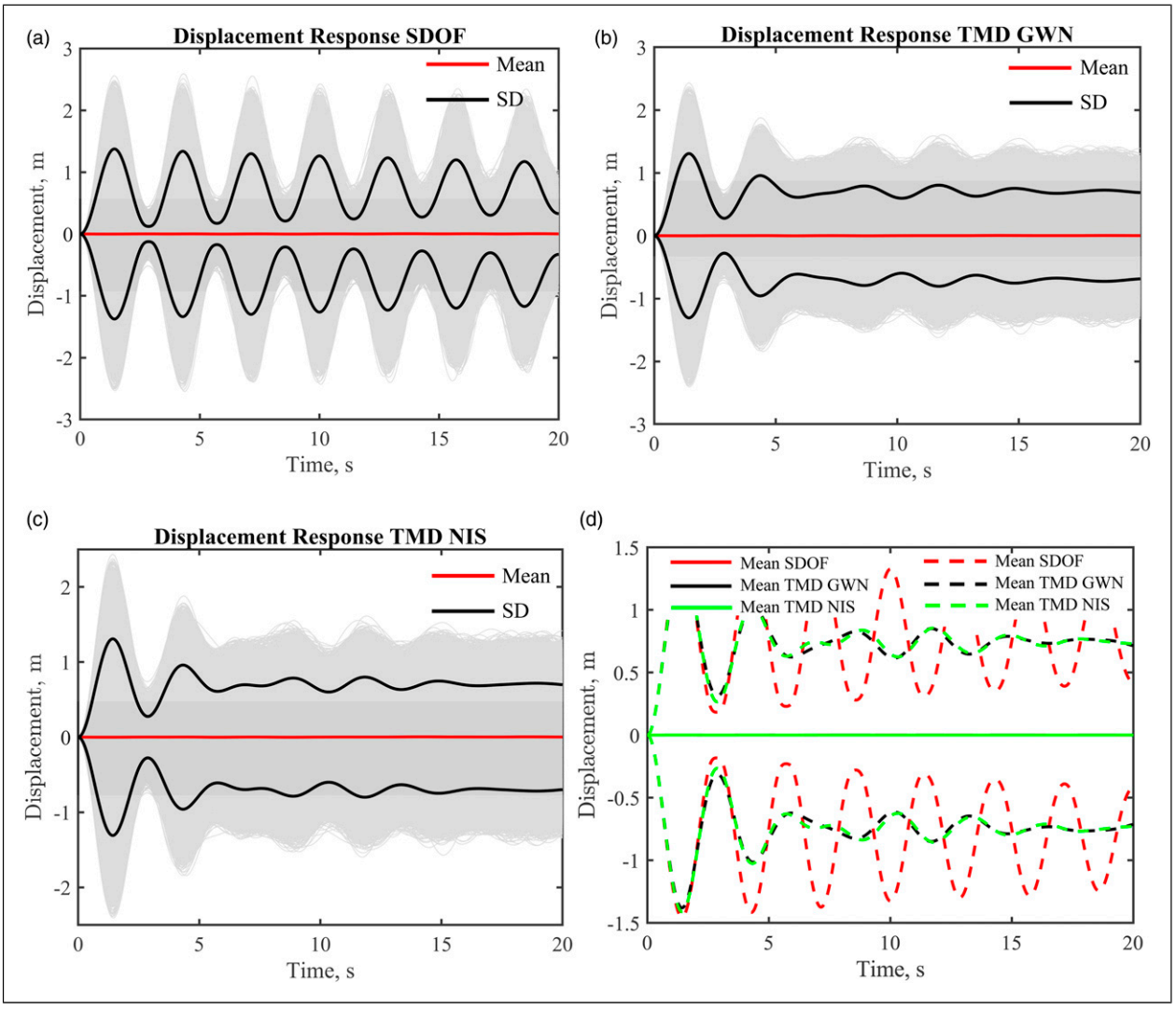

Figure 8. (a), (b) and (c) Time displacement curve including mean and standard deviation for SDOF, TMD optimized for GWN and TMD optimized for NIS subjected to KS and (d) mean and standard deviation comparison between all the three cases subjected to KS.

Table 1. Geometric, material and wind load properties for Siemens SWT-107-3.6 offshore wind turbine (Arany et al., 2015).

Property	Symbols	Values
Diameter of the rotor (m)	D	107
Density of air (kg/m^3)	ρ_a	1.225
Mean wind speed (m/s)	U	9
Turbulence intensity	I	0.1
Integral length scale	L_k	340.2
Drag coefficient	C_D	0.5
Young's modulus of the tower material (GPa)	E	210
Tower height (m)	L	5.0
Bottom Diameter (m)	D_b	5.0
Top Diameter (m)	D_t	3.0
Tower wall thickness (mm)	t	50
Tower mass (kg)	M_t	260000
Rotor nacelle assembly (RNA) mass (kg)	M_{RNA}	234500
Lateral foundation stiffness (GNm^{-1})	K_L	3.65
Rotational foundation stiffness (GNmrad^{-1})	K_R	254.3

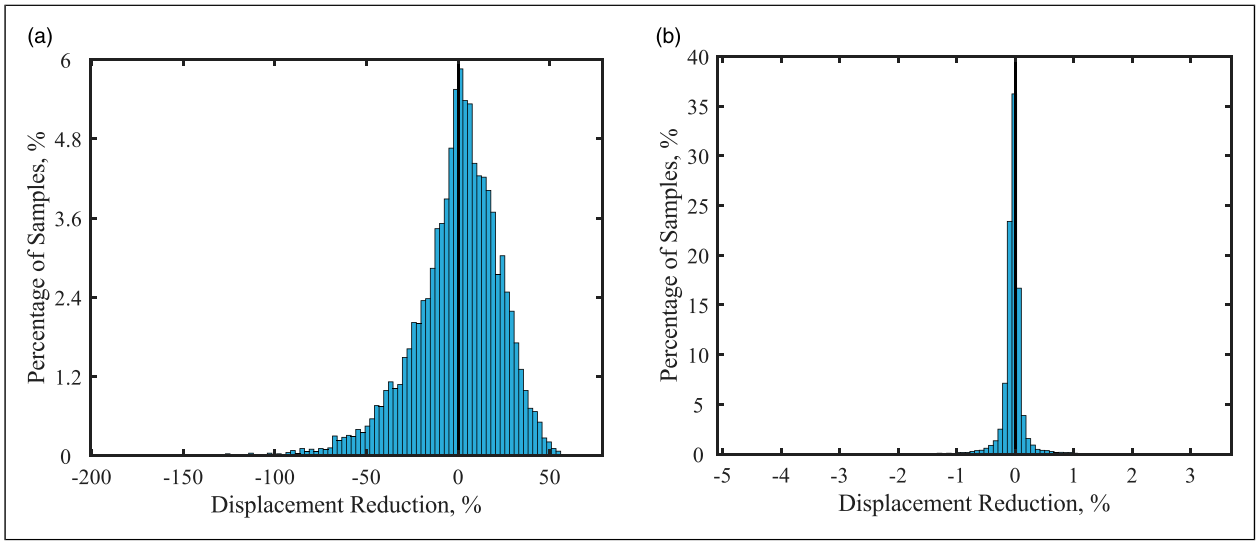

Figure 9. (a) and (b) Histogram plot for performance reduction when the system subjected to GWN and KS.

TMD NIS is difficult to obtain from Figure 7 (d) and Figure 8 (d). Thus, to omit the confusion, histogram plots has been made for the response reduction between TMD optimized through GWN and TMD optimized through NIS subjected to GWN and the Kaimal spectrum considering the same sample size of 10,000 as shown in Figure 9 (a and b). Here, the response reduction can be defined as

$$RR(\%) = \frac{y_{normKS} - y_{normGWN}}{y_{normKS}} \times 100 \tag{23}$$

where $y_{normGWN}$ = L_2 norm or root mean square of the displacement responses of the TMD system is optimized by Gaussian white noise, and $y_{normKS} = L_2$ norm or root mean square of the displacement responses of the TMD system is optimized by the Kaimal spectrum. When the TMD is subjected to Gaussian white noise, then the histogram of response reduction is more inclined towards positive side; in other words, positive area is more than negative area as shown in Figure 9 (a), whereas when the TMD system is subjected to the Kaimal spectrum, then the response reduction is more inclined towards the negative side or more negative area as shown in Figure 9(b). This clearly indicates that if the system is subjected to Gaussian white noise, then displacement response will be minimum when optimized according to GWN. Similarly, if the system is subjected to the Kaimal spectrum, then displacement response will be minimum when optimized according to the Kaimal spectrum.

4. Conclusion

A classical mechanics-based methodology towards the estimation of optimum parameters of a tuned mass damper (TMD) system subjected to the Kaimal Spectrum using the H_2 optimization technique has been communicated in this paper. The optimal parameters of a TMD is obtained by minimizing the standard deviation of the displacement response which is known as the H_2 optimization technique. A validation study has been conducted with the existing literature for the TMD system subjected to Gaussian white noise (GWN). Obtaining an analytical closed-form expression of the objective function for a TMD system considering a real spectrum, having fractional order of the frequency, is very challenging. Therefore, usually objective functions are obtained numerically which does not directly yield the optimum point and increase the computational cost significantly. To deal with the aforementioned challenges associated with the fractional power of excitation frequency in the power spectral density, a concept of near identity spectrum (NIS) has been proposed. The NIS contains excitation frequency as a product of complex conjugate which enables us to form a closed-form expression of the objective function. The proposed NIS precisely matches with the Kaimal spectrum; hence, it omits the fractional power in the variance equation. The closed-form analytical expression of the objective function can be directly plotted to obtain the optimal parameters of the TMD system. A sample of 10,000 time histories obtained from GWN and the Kaimal spectrum are applied to the system as in input force to realize the performance of the optimized TMD. From the histogram plot, it can be concluded that minimum displacement response occurs while the system can be optimized according to the input forcing spectrum rather than any other noise/spectrum. Thus, the novelty lies in proposing a NIS that can be used as a generalized

spectrum to estimate the optimum parameters of the TMD system implementing the H_2 optimization technique. Due to severe change in climatic condition in recent years, the demand of stable, clean and green energy production becomes the primary mission of several countries. Towards this mission, the developed NIS contributed for easy simulation of wind load and provides a generalized method for optimal design which can be used in design firms for next generation wind turbine design and control. Further, this concept of NIS could be extended in the future study to generalize other dynamic loads, such as wave loads and earthquake loads.

6. Annexure

The values of $T(\lambda)$, M_6, Δ_6 and derivation of the integral in equation (20) are listed below

$$T(\lambda) = \frac{B_0(i\lambda)^3 + B_1(i\lambda)^2 + B_2(i\lambda) + B_3}{\begin{pmatrix} A_0(i\lambda)^6 + A_1(i\lambda)^5 + A_2(i\lambda)^4 \\ +A_3(i\lambda)^3 + A_4(i\lambda)^2 + A_5(i\lambda) \\ +A_6 \end{pmatrix}}, \tag{24}$$

in which

$$B_0 = \varepsilon, \tag{25}$$

$$B_1 = 2v\varepsilon\zeta_2 + 1, \tag{26}$$

$$B_2 = \varepsilon v^2 + 2\zeta_2 v, \tag{27}$$

$$B_3 = v^2, \tag{28}$$

$$A_0 = \chi\phi, \tag{29}$$

$$A_1 = \chi + \phi + 2\chi\phi\zeta_1 + 2\chi v\phi\zeta_2 + 2\chi\mu v\phi\zeta_2, \tag{30}$$

$$A_2 = \begin{pmatrix} \chi\phi + 2\chi\zeta_1 + 2\phi\zeta_1 + \chi v^2\phi + 2\chi v\zeta_2 \\ +2v\phi\zeta_2 + 2\chi\mu v\zeta_2 + 2\mu v\phi\zeta_2 + \chi\mu v^2 v \\ +4\chi v\phi\zeta_1\zeta_2 + 1 \end{pmatrix}, \tag{31}$$

$$A_3 = \begin{pmatrix} \chi + \phi + 2\zeta_1 + 2v\zeta_2 + \chi v^2 + \\ v^2\phi + \mu v^2\phi + 2\mu v\zeta_2 + \chi\mu v^2 + \\ 2\chi v\phi\zeta_2 + 4\chi v\zeta_1\zeta_2 + 4v\phi\zeta_1\zeta_2 + 2\chi v^2\phi\zeta_1 \end{pmatrix}, \tag{32}$$

$$A_4 = \begin{pmatrix} \mu v^2 + v^2 + \chi v^2\phi + 2\chi v^2\zeta_1 + 2v^2\phi\zeta_1 \\ +2\chi v\zeta_2 + 2v\phi\zeta_2 + 4v\zeta_1\zeta_2 + 1 \end{pmatrix}, \tag{33}$$

$$A_5 = 2v\zeta_2 + \chi v^2 + v^2\phi + 2v^2\zeta_1 \tag{34}$$

and

$$A_6 = v^2 \tag{35}$$

To evaluate equation (20), James et al. (1947) suggested a method in which the integrand must be in the form of

$$I_n = \frac{1}{2\pi j}\int_{-\infty}^{\infty} \frac{g_n(x)}{h_n(x)h_n(-x)}dx \tag{36}$$

where

$$g_n(x) = b_0x^{2n-2} + b_1x^{2n-4} + \cdots + b_{n-1} \tag{37}$$

and

$$h_n(x) = a_0x^n + a_1x^{n-1} + \cdots + a_n \tag{38}$$

Now by assuming $q = i\lambda$ and writing integrand of equation (20) in form of integrand of equation (36), we get as follows

$$\frac{g_6(x)}{h_6(x)h_6(-x)} = \frac{\begin{pmatrix} C_0x^6 + C_1x^4 + \\ C_2x^2 + C_3 \end{pmatrix}}{\left\{\begin{pmatrix} A_0x^6 + A_1x^5 + A_2x^4 \\ +A_3x^3 + A_4x^2 + A_5x \\ +A_6 \end{pmatrix}\right\}\left\{\begin{pmatrix} A_0x^6 - A_1x^5 + A_2x^4 \\ -A_3x^3 + A_4x^2 - A_5x \\ +A_6 \end{pmatrix}\right\}} \tag{39}$$

where

$$C_0 = -u^2 \tag{40}$$

$$C_1 = (2vu\zeta_2 + 1)^2 - 2u\left(uv^2 + 2\zeta_2 v\right) \tag{41}$$

$$C_2 = 2(2vu\zeta_2 + 1)v^2 - \left(uv^2 + 2\zeta_2 v\right)^2 \tag{42}$$

and

$$C_3 = v^4 \tag{43}$$

Since the highest power of x in equation (39) is 6, thus, by substituting $n = 6$ in equation (36), (37) and (38), we obtain the integrand as

$$\frac{g_6(x)}{h_6(x)h_6(-x)} = \frac{\begin{pmatrix} b_0x^{10} + b_1x^8 + b_2x^6 + b_3x^4 \\ +b_4x^2 + b_5 \end{pmatrix}}{\left\{ \begin{pmatrix} a_0x^6 + a_1x^5 + a_2x^4 + \\ a_3x^3 + a_4x^2 + a_5x + a_6 \end{pmatrix} \begin{pmatrix} a_0x^6 - a_1x^5 + a_2x^4 - \\ a_3x^3 + a_4x^2 - a_5x + a_6 \end{pmatrix} \right\}} \quad (44)$$

Now, comparing equations (39) and (44), we obtain the coefficients as $b_0 = b_1 = 0$, $b_2 = C_0$, $b_3 = C_1$, $b_4 = C_2$, $b_5 = C_3$ and $a_i = A_i$, where $i = 1$ to 6. Thus, equation (20) can be evaluated as

$$\sigma_{xx}^2 = 2\pi\alpha\omega_1 \times \frac{1}{2\pi j}\int_{-\infty}^{\infty} \frac{g_6(x)}{h_6(x)h_6(-x)}dx = \frac{\pi\alpha\omega_1 M_6}{a_0\Delta_6} \quad (45)$$

where

$$M_6 = \begin{pmatrix} b_0d_0 + a_0b_1d_1 + a_0b_2d_2 + \\ a_0b_3d_3 + a_0b_4d_4 + \dfrac{a_0b_5}{a_6}d_5 \end{pmatrix} \quad (46)$$

and

$$\Delta_6 = \begin{pmatrix} a_0^2a_5^3 + 3a_0a_1a_3a_5a_6 - 2a_0a_1a_4a_5^2 - \\ a_0a_2a_3a_5^2 - a_0a_3^3a_6 + a_0a_3^2a_4a_5 + a_1^3a_6^2 - \\ 2a_1^2a_2a_5a_6 - a_1^2a_3a_4a_6 + a_1^2a_4^2a_5 + a_1a_2^2a_5^2 + \\ a_1a_2a_3^2a_6 - a_1a_2a_3a_4a_5 \end{pmatrix} \quad (47)$$

where

$$d_0 = \begin{pmatrix} -a_0a_3a_5a_6 + a_0a_4a_5^2 - a_1^2a_6^2 + 2a_1a_2a_5a_6 \\ +a_1a_3a_4a_6 - a_1a_4^2a_5 - a_2^2a_5^2 - a_2a_3^2a_6 \\ +a_2a_3a_4a_5 \end{pmatrix}, \quad (48)$$

$$d_1 = -a_1a_5a_6 + a_2a_5^2 + a_3^2a_6 - a_3a_4a_5, \quad (49)$$

$$d_2 = -a_0a_5^2 - a_1a_3a_6 + a_1a_4a_5, \quad (50)$$

$$d_3 = a_0a_3a_5 + a_1^2a_6 - a_1a_2a_5, \quad (51)$$

$$d_4 = a_0a_1a_5 - a_0a_3^2 - a_1^2a_4 + a_1a_2a_3 \quad (52)$$

and

$$d_5 = \begin{pmatrix} a_0^2a_5^2 + a_0a_1a_3a_6 - 2a_0a_1a_4a_5 \\ -a_0a_2a_3a_5 + a_0a_3^2a_4 - a_1^2a_2a_6 + a_1^2a_4^2 \\ +a_1a_2^2a_5 - a_1a_2a_3a_4 \end{pmatrix} \quad (53)$$

Acknowledgements

Authors like to acknowledge the research grant, namely Core research grant, Science and Engineering Research Board, Department of Science and Technology, Ministry of Science and Technology, Government of India, grant number CRG/2019/004696 for partial financial support for the research.

Declaration of conflicting interests

The author(s) declared no potential conflicts of interest with respect to the research, authorship, and/or publication of this article.

Funding

The author(s) disclosed receipt of the following financial support for the research, authorship, and/or publication of this article: Science and Engineering Research Board (CRG/2019/004696).

ORCID iD

Arnab Banerjee https://orcid.org/0000-0002-3157-6200

References

Adhikari S and Banerjee A (2021) Enhanced low-frequency vibration energy harvesting with inertial amplifiers. *Journal of Intelligent Material Systems and Structures* 33: 822–838.

Adhikari S and Bhattacharya S (2011) Vibrations of wind-turbines considering soil-structure interaction. *Wind and Structures* 14(2): 85–112.

Adhikari S, Friswell M, Litak G, et al. (2016) Design and analysis of vibration energy harvesters based on peak response statistics. *Smart Materials and Structures* 25(6): 065009.

Anh N and Nguyen NX (2014) Design of non-traditional dynamic vibration absorber for damped linear structures. *Proceedings of the Institution of Mechanical Engineers, Part C: Journal of Mechanical Engineering Science* 228(1): 45–55.

Ankireddi S and Yang YHT (1996) Simple atmd control methodology for tall buildings subject to wind loads. *Journal of Structural Engineering* 122(1): 83–91.

Arany L, Bhattacharya S, Macdonald J, et al. (2015) Simplified critical mudline bending moment spectra of offshore wind turbine support structures. *Wind Energy* 18(12): 2171–2197.

Asami T, Hosokawa Y (1995) Approximate expression for design of optimal dynamic absorbers attached to damped linear systems (2nd report, optimization process based on the fixed-points theory). *Transactions of the Japan Society of Mechanical Engineers, Series C* 61(583): 915–922.

Asami T, Nishihara O and Baz AM (2002) Analytical solutions to h_∞ and h_2 optimization of dynamic vibration absorbers attached to damped linear systems. *Journal of Vibration and Acoustics* 124(2): 284–295.

Asami T, Nishihara O, Baz AM, et al. (2001) Closed-form exact solution to H_2 optimization of dynamic vibration absorbers attached to damped linear systems. *Transactions of the Japan Society of Mechanical Engineers Series C* 67(655): 597–603.

Asami T, Wakasono T, Kameoka K, et al. (1991) Optimum design of dynamic absorbers for a system subjected to random excitation. *JSME International Journal. Ser. 3, Vibration, Control Engineering, Engineering for Industry* 34(2): 218–226.

Brock JE (1946) A note on the damped vibration absorber. *Journal of Applied Mechanics* 13: A284–A284.

Cheung Y and Wong W (2009) Design of a non-traditional dynamic vibration absorber. *The Journal of the Acoustical Society of America* 126(2): 564–567.

Cheung Y and Wong WO (2011) H_2 optimization of a non-traditional dynamic vibration absorber for vibration control of structures under random force excitation. *journal of Sound and Vibration* 330(6): 1039–1044.

Chowdhury S, Banerjee A and Adhikari S (2021).Enhanced seismic base isolation using inertial amplifiers. *Structures* 33: 1340–1353.

Chowdhury S, Banerjee A and Adhikari S (2022) Optimal negative stiffness inertial-amplifier-base-isolators: Exact closed-form expressions. *International Journal of Mechanical Sciences* 218: 107044

Chun S, Lee Y and Kim TH (2015) H_∞ optimization of dynamic vibration absorber variant for vibration control of damped linear systems. *Journal of Sound and Vibration* 335: 55–65.

Colwell S. and Basu B. (2009) Tuned liquid column dampers in offshore wind turbines for structural control. *Engineering Structures* 31: 358–368.

International Electrotechnical Commission. (2005). Wind turbines-part 1: design requirements. IEC 61400-1 Ed. 3, Geneva, Switzerland: International Electrochemical Commission.

Den Hartog JP (1985) *Mechanical Vibrations*. North Chelmsford, MA: Courier Corporation.

Det N (2013) Dnv offshore standard dnv-os-j101, design of offshore wind turbine. *Technical Standard*: 134–135.

Frohboese P, Schmuck C and Hassan GG (2010) Thrust coefficients used for estimation of wake effects for fatigue load calculation, European Wind Energy Conference, Warsaw, Poland, April, 2010

Ghosh A. and Basu B. (2007) A closed-form optimal tuning criterion for TMD in damped structures. *Structural Control and Health Monitoring* 14(4): 681–692.

Hahnkamm E (1933) Die dämpfung von fundamentschwingungen bei veränderlicher erregerfrequenz. *Ingenieur-Archiv* 4(2): 192–201.

Ioi T and Ikeda K (1978) On the dynamic vibration damped absorber of the vibration system. *Bulletin of JSME* 21(151): 64–71.

James HM, Nichols NB and Phillips RS (1947) *Theory of Servomechanisms*. New York: McGraw-Hill, 25.

Li Y, Zhu L, Qian C, et al. (2021) The time-varying modal information of a cable-stayed bridge: some consideration for SHM. *Engineering Structures* 235: 111835.

Liu K and Coppola G (2010) Optimal design of damped dynamic vibration absorber for damped primary systems. *Transactions of the Canadian Society for Mechanical Engineering* 34(1): 119–135.

Liu K and Liu J (2005) The damped dynamic vibration absorbers: revisited and new result. *Journal of Sound and Vibration* 284(3–5): 1181–1189.

Newland D (1993) *An Introduction to Random Vibrations, Spectral and Wavelet Analysis*. Essex, England: Longman Scientific & Technical.

Nishihara O and Matsuhisa H (1997) Design and tuning of vibration control devices via the stability criterion. *Preparation of the Japan Society of Mechanical Engineering* 97: 165–168.

Ormondroyd J (1928) The theory of the dynamic vibration absorber. *Trans., ASME, Applied Mechanics* 50: 9–22.

Randall S, Halsted D, III and Taylor D (1981) Optimum vibration absorbers for linear damped systems. *Journal of Mechanical Design* 103: 908–913.

Ren M (2001) A variant design of the dynamic vibration absorber. *Journal of Sound and Vibration* 245(4): 762–770.

Sekiguchi H and Asami T (1984) Theory of vibration isolation of a system with two degrees of freedom: 1st report, motion excitation. *Bulletin of JSME* 27(234): 2839–2846.

Snowdon J (1974) Dynamic vibration absorbers that have increased effectiveness. *Journal of Manufacturing Science and Engineering* 96: 940–945.

Soom A and Lee Ms (1983) Optimal design of linear and nonlinear vibration absorbers for damped systems. *Journal of Vibration and Acoustics* 105: 112–119.

Thompson A (1981) Optimum tuning and damping of a dynamic vibration absorber applied to a force excited and damped primary system. *Journal of Sound and Vibration* 77(3): 403–415.

Tian L and Gai X (2015) Wind-induced vibration control of power transmission tower using pounding tuned mass damper. *Journal of Vibroengineering* 17(7): 3693–3701.

Tsai HC and Lin GC (1993) Optimum tuned-mass dampers for minimizing steady-state response of support-excited and damped systems. *Earthquake Engineering & Structural Dynamics* 22(11): 957–973.

Warburton G (1982) Optimum absorber parameters for various combinations of response and excitation parameters. *Earthquake Engineering & Structural Dynamics* 10(3): 381–401.

Wong WO and Cheung Y (2008) Optimal design of a damped dynamic vibration absorber for vibration control of structure excited by ground motion. *Engineering Structures* 30(1): 282–286.

Yamaguchi H and Harnpornchai N (1993) Fundamental characteristics of multiple tuned mass dampers for suppressing harmonically forced oscillations. *Earthquake Engineering & Structural Dynamics* 22(1): 51–62.

Zuo L (2009) Effective and robust vibration control using series multiple tuned-mass dampers. *Journal of Vibration and Acoustics* 131(3).